Automatic Measurement of Thyroid Gland

Eystratios Keramidas[1], Dimitris Iakovidis[1], Dimitris Maroulis[1],
and Nikos Dimitropoulos[2]

[1] Dept. of Informatics and Telecommunications, University of Athens, Greece
[2] Medical School of the University of Athens, Greece.
rtsimage@di.uoa.gr, dimitris.iakovidis@ieee.org

Abstract

This study presents a novel method for automatic measurement of the anteroposterior diameter of the thyroid gland, in ultrasound images. Anteroposterior diameter is widely considered a basic parameter for goiter assessment. Goiter refers to abnormal enlargement of the thyroid gland and it is associated with iodine deficiency and various pathologic conditions including Hashimoto's thyroiditis, and growing nodules. The proposed method is based on processing local histogram information extracted from vertically sampled horizontal image stripes. The anteroposterior diameter can be derived by measuring the distance between the hyperechoic lines that bound the thyroid lobes as depicted in longitudinal ultrasound images. Extensive experiments were carried out on a set of B-mode thyroid ultrasound images, in order to evaluate the effectiveness of the proposed method. The results advocate to the feasibility of its use for objective measurement of the anteroposterior diameter of the thyroid gland.

Keywords: Computer-Aided Measurement, Thyroid, Ultrasound, Local Histogram, Anteroposterior Diameter

1. Introduction

Thyroid gland is one of the larger endocrine glands, which secretes hormones to regulate physiological functions in human's body. According to population surveys, an enlarged thyroid has been observed in more than 18% of the examined population [Reiners et. Al. (2004)]. Growth or enlargement of thyroid, called goiter, is closely related to a number of different conditions including iodine deficiency, Hashimoto's thyroiditis, Graves' disease, growing nodules, tumors, genetic defects, and injuries or infections in thyroid gland [Mickuviene et. Al. (2006)] [Tajiri (2006)] [Juan (2005)] [Gillam et. Al. (2001)]. In particular, goiter size determination is used for assessing the need for surgery, for the calculation of the dose of I^{131} needed for treating thyrotoxicosis, and for the evaluation of the response to suppression treatments. A medical examination that is widely used for goiter size determination is B-mode ultrasonography. A common practice for goiter assessment is to measure the anteroposterior (AP) diameter of the thyroid gland manually using the cursors provided by ultrasound devices [Rumack et. Al. (2004)]. However, such a manual

measurement is susceptible to subjectivity and errors. An automatic image analysis method would be regarded as an approach towards the objectification of the measurement of the AP diameter.

A variety of ultrasound image analysis methods for automatic assessment of the status of human organs, including heart, liver, kidney, breast, prostate, and thyroid have been proposed [Yoshida et. Al. (2003)] [Kutay et. Al. (2003)] [Noble et. Al. (2006)] [Llobet et. Al. (2006)]. Early approaches to thyroid ultrasound image analysis utilize local grey-level histogram information for the characterization of the histological state of the thyroid tissue and for the identification of Hashimoto disease [Mailloux et. Al. (1985)]. Subsequent approaches are based on spatial, first and second order statistical features as well as frequency domain features for computer aided diagnosis of lymphocytic thyroiditis (LT) [Smutek et. Al. (2003)]. Recent approaches aim to the delineation of thyroid nodules using active contours [Iakovidis et. Al. (2006)]. However, there is no published work dealing with the detection of thyroid boundaries and the measurement of the AP diameter of the thyroid gland.

In this paper, we propose a novel method for automatic measurement of the AP diameter. This method is based on processing local histogram information to detect the boundaries of the thyroid gland. The AP diameter can be derived by measuring the distance between these boundaries. The advantages of this method include noise robustness and low computational complexity.

The rest of this paper is organized in four sections. Section 2 describes the proposed method for the detection of the thyroid boundaries, which can be used to measure the AP diameter of the thyroid gland. In Section 3 a description of the experimental procedures followed along with results derived are presented. Finally, the conclusions as well as future perspectives of this study are summarized in Section 4.

2. Detection of thyroid boundaries

Thyroid parenchyma is bounded by thin hyperechoic lines, which are identifiable in longitudinal ultrasound images. These hyperechoic lines can be detected as follows:

Step 1: A normalized ultrasound input image of $N \times M$ pixels and G grey levels, is uniformly quantized into z discrete grey levels. Grey level quantization results in a rough segmentation of the image and accentuates the hyperechoic bounds of the thyroid gland (Fig. 1b).

Step 2: The quantized image is vertically scanned from top to bottom with horizontal stripes of h pixels height, and M pixels width. Between each two successive stripes a step of $s \in (0, h]$ pixels is applied, as depicted in Fig. 1c, resulting to a total of K successive stripes.

(a)   (b)

(c)   (d)
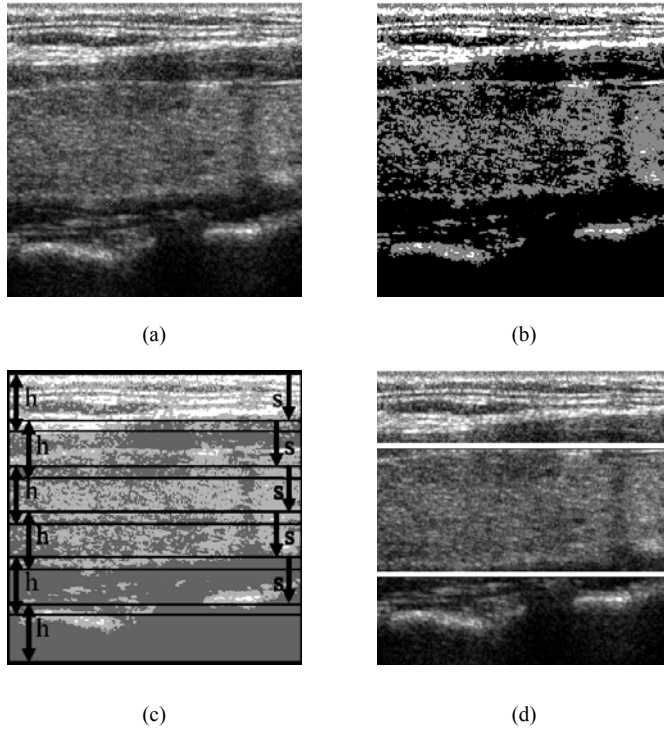
Figure 1. *a) The original longitudinal ultrasound image of thyroid gland with G=256 grayscale levels (b) The quantized ultrasound image of z=3 grey levels.(c) The quantized image with K horizontal stripes of height h and step s. (d) The original image with thyroid boundaries drawn by the proposed method.*

Step 3: The weighted sum I_n of the number of pixels with grey level j, that belong to each stripe n of the quantized image, is calculated by the following equation:

$$I_n = \sum_{j=0}^{G} \left(w(j) \cdot \sum_{P_{j,n}} 1 \right) \tag{1}$$

where n is a stripe index incrementing from top ($n = 1$) to bottom ($n = K$) and $P_{j,n}$ represents the set of pixels having grey level j and reside within stripe n. A quadratic weight function $w(j) = a \cdot j^2 + \beta \cdot j + \gamma$, where α, β, γ are constants, has been considered so as to amplify the contribution of higher grey levels in the calculation of I_n. Constants β, γ are chosen so as to satisfy $(w, j) = (0, 0)$ and $(w, j) = (1, G)$, therefore $w(j)$ is finally derived by the following equation:

$$w(j) = a \cdot j^2 + \frac{1 - a \cdot G^2}{G} j \tag{2}$$

Such amplification aims to the enhancement of the grey levels representing thyroid boundaries, which appear as hyperechoic lines.

Step 4: For each stripe the derivative of I_n, multiplied by I_n is estimated by Eq. (3). This equation represents the rate of change of I_n, between two successive stripes and emphasizes on I_n 's with high values.

$$D_n = \left. \frac{d(I_i)}{di} \right|_{i=n} \cdot I_n , \ \ n = 1,2,...K \tag{3}$$

Step 5: The outer and the inner thyroid boundaries can be located by identifying the stripes for which the following conditions are satisfied:

$$\begin{cases} n_{outer} = \arg\min_n [D_n \cdot \omega_1(n)] \\ n_{inner} = \arg\max_n [D_n \cdot \omega_2(n)] \\ n_{inner} - n_{outer} > \dfrac{T}{h}, \quad \text{where } T > 0 \end{cases} \tag{4}$$

$$\omega_1(n) = \begin{cases} \log\left(\dfrac{\lambda \cdot K - n}{\lambda \cdot K} + 1 \right) & n < \lambda \cdot K \\ 0 & n \ge \lambda \cdot K \end{cases} \tag{5}$$

$$\omega_2(n) = \begin{cases} \log\left(\dfrac{n - (1 - \lambda) \cdot K}{\lambda \cdot K} + 1 \right) & n < (1 - \lambda) \cdot K \\ 0 & n \ge (1 - \lambda) \cdot K \end{cases} \tag{6}$$

$$\lambda = 1 - \frac{T}{N} \tag{7}$$

where n_{outer} and n_{inner} are the stripe indices that correspond to the outer and the inner boundaries respectively (Fig. 1c, indicated by thick lines). Threshold T represents a minimum AP diameter and ensures that stripe n_{outer} will always reside below stripe n_{inner}. The logarithmic weight functions $\omega_1(n)$ and $\omega_2(n)$ are used to bias n_{outer} and n_{inner} towards the upper and lower image areas, respectively.

3. Results

Extensive experiments were performed with a variety of real thyroid ultrasound images to investigate the performance of the proposed method. Thyroid ultrasound examinations were performed using a digital ultrasound imaging system HDI 3000 ATL with a 5-12 MHz linear transducer at the Department of Radiology of Euromedica, Greece. A total of 39 longitudinal in vivo digital thyroid images were acquired at a resolution of 256×256 pixels with 256 grey-level depth. The dataset

used in the experiment is comprised of different thyroid cases, including healthy, enlarged and nodular.

Three expert radiologists marked manually thyroid lobe bounds, on the available ultrasound images. Each radiologist determined the AP diameter of the thyroid gland using a single point mark for each side of the thyroid lobe (Fig. 2a).

Images facilitating ground truth AP diameter estimation were generated as follows: a) the marks designated by the radiologists were extended over the whole image width forming two parallel horizontal lines; b) an image row belongs to the region within the thyroid boundaries only if it lies between the two horizontal lines defined by the marks of at least two out of three experts [Kaus et. Al. (1999)]. As a measure of accuracy for AP diameter estimation we consider the overlap between the region corresponding to the ground truth AP diameter and the region corresponding to the AP diameter estimated by the proposed method.

| (a) | (b) | (c) |
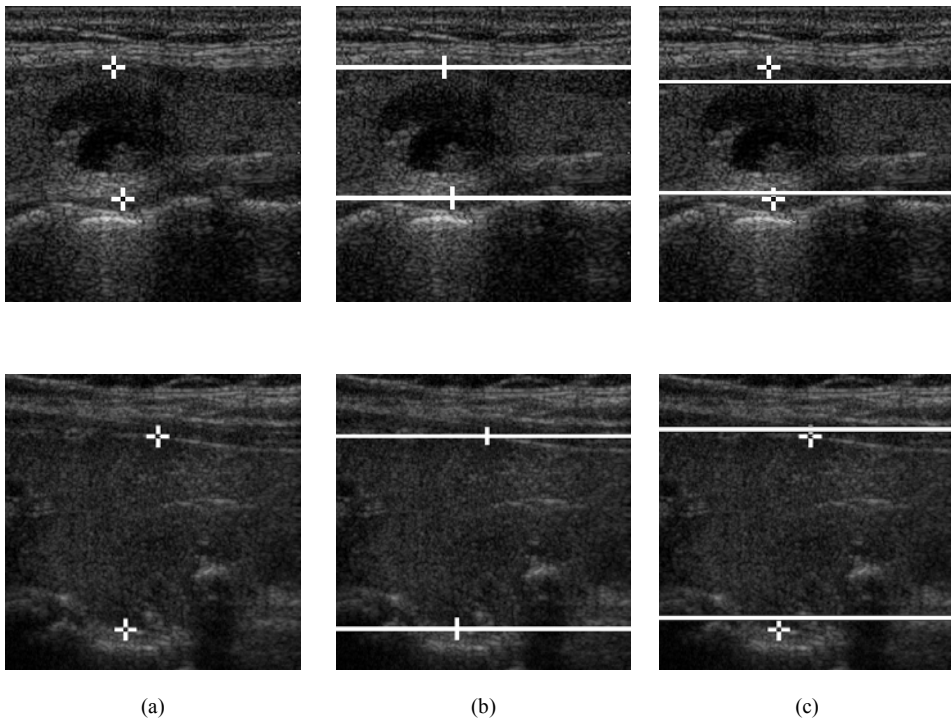
Figure 2. *(a) Two sample thyroid ultrasound images marked by radiologists, (b) image region defined by the radiologists' marks, (c) image region defined by the proposed method.*
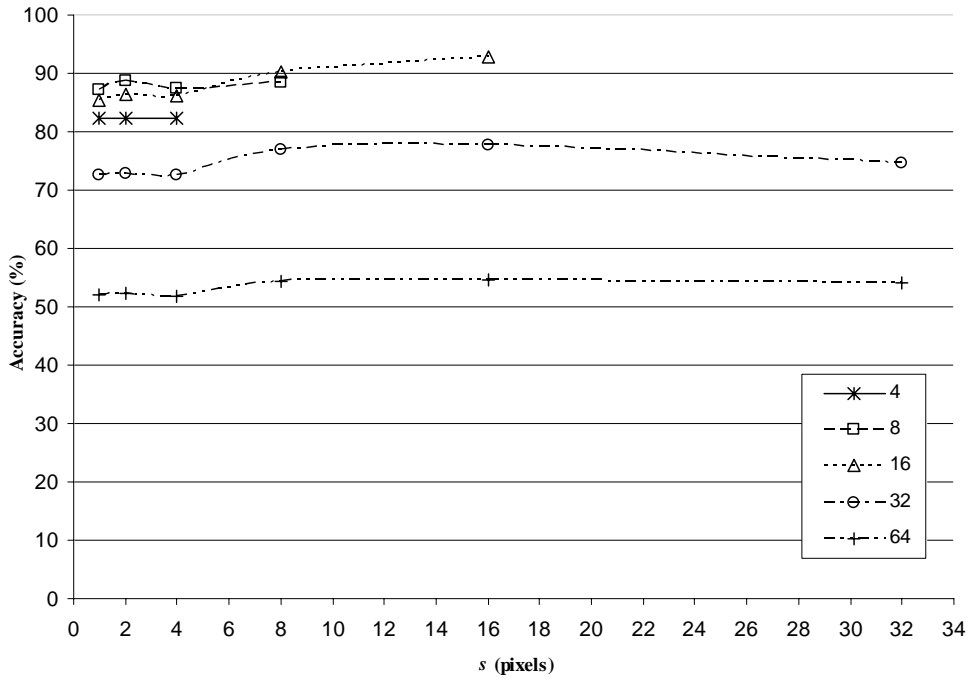
Figure 3. *Mean accuracy of the proposed method for different values of h and s parameters.*
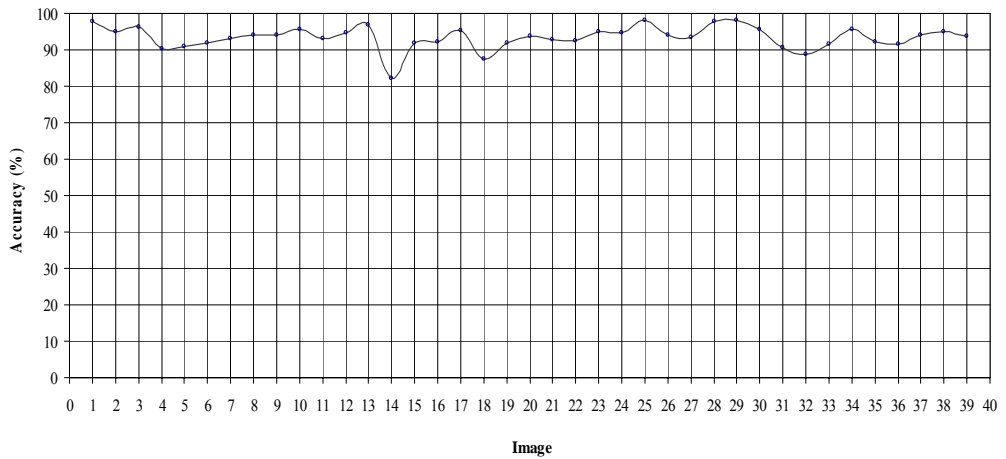
Figure 4. *Accuracy of the proposed method on each ultrasound image for h= 16 and s=16.*

In order to determine the optimal stripe dimensions, that minimize the error between the diameter estimated with the proposed method and the ground truth, we performed exhaustive experiments for $h \in H$ and $s \in H$: $s \leq h$, where $H = \{4, 8, 16, 32, 64\}$. The optimal values of the investigated parameters are $h=16$ and $s=16$ pixels, for which the mean accuracy in the measurement of the AP diameter reaches a maximum of 93.2±3.0%.

The results illustrated in Fig 3 show that for large h the proposed method leads to gross detection of the boundaries, resulting in diminution of AP measurement accuracy. For stripe step s, experiments suggest that higher accuracies can be obtained for larger values of s. Larger step values s, result in less common pixels between successive stripes, which leads to more rigorous computation of I_n.

The accuracy of the proposed method per image for the optimal parameters is illustrated in Fig. 4. This figure shows that in 35 out of 39 cases, i.e. for 92.3% of the available images the accuracy exceeds 90.0%. The accuracy falls below 90% for images in which the thyroid boundaries are either not clearly visible or invisible. Such cases usually occur due to low acoustic power and intensity of the ultrasound transducer.

4. Conclusions

A novel, unsupervised, low complexity method for the measurement of the anteroposterior diameter of the thyroid gland was presented. This method utilizes local statistical properties of the ultrasound images inherently affected by speckle noise. It was applied for computer-aided measurement of the AP diameter of the thyroid gland in real ultrasound images.

The results of the experimental study presented in this paper lead to the following conclusions about the proposed method:

- Its performance is comparable to that of expert radiologists.
- It exhibits high accuracy for a wide range of cases including both normal and pathologic conditions.
- It contributes to the objectification of the AP measurement process by utilizing explicit image features.
- It provides the diagnosticians with a second opinion on the assessment of goiter.
- Its application in clinical practice is feasible and could contribute to the reduction of false medical decisions.

Future perspectives of this work include:

- Enhancement of the functionality of the proposed method, to deal with ultrasound images in which the thyroid boundaries are not clearly visible or invisible.
- Evolvement of the proposed method for volumetric assessment of the thyroid gland.

Acknowledgment

References

Gillam MP., Kopp P. (2001), *Genetic defects in thyroid hormone synthesis*, Current Opinion in Pediatrics, vol. 13, pp. 364-372.

Iakovidis D.K., Savelonas M.A., Karkanis S.A., Maroulis D.E. (2006). *Segmentation of Medical Images with Regional Inhomogeneities*, Proc. International Conference on Pattern Recognition (ICPR), IAPR, Hong Kong, vol. 2, pp. 279-282.

Juan J.D. (2005), *Goiter in Adult Patients Aged 55 Years and Older: Etiology and Clinical Features in 634 Patients*, The Journals of Gerontology Series A: Biological Sciences and Medical Sciences vol. 60, pp. 920-923.

Tajiri. J. (2006), *Radioactive Iodine Therapy for Goitrous Hashimoto's Thyroiditis*, Journal of Clinical Endocrinology & Metabolism, vol. 91, pp. 4497-4500.

Kaus M.R., Warfield S.K., Jolesz F.A., Kikinis R. (1999), *Segmentation of Meningiomas and Low Grade Gliomas in MRI*, Proc. Second International Conference on Medical Image Computing and Computer-Assisted Intervention, Cambridge, England, vol. 1679, pp. 1-10.

Kutay M.A., Petropulu A.P., Piccoli C.W. (2003), *Breast tissue characterization based on modeling of ultrasonic echoes using the power-law shot noise model*, Pattern Recognition Letters, vol. 24, pp. 741–756.

Llobet R., Perez-Cortes J.C., Toselli A.H., Juan A. (2006), *Computer-aided detection of prostate cancer*, International Journal of Medical Informatics.

Mailloux G.E., Bertrand M., Stampfler R. (1985), *Local Histogram Information Content Of Ultrasound B-Mode Echographic Texture*, Ultrasound in Medicine and Biology, vol. 11, pp. 743-50.

Mickuviene N., Krasauskiene A., Kazanavicius G. (2006), *The results of thyroid ultrasound examination in randomly selected schoolchildren*, Medicina, vol. 42, pp. 751-758.

Noble J., Boukerroui D. (2006), *Ultrasound Image Segmentation: A Survey*, Medical Imaging, IEEE Transactions on, vol. 25, pp. 987-1010.

Reiners C., Wegscheider K., Schicha H., Theissen P., Vaupel R., Wrbitzky R., Schumm-Draeger PM. (2004), *Prevalence of thyroid disorders in the working population of Germany: ultrasonography screening in 96,278 unselected employees*, Thyroid : official journal of the American Thyroid Association, vol. 14, pp. 879-880.

Rumack C.M., Wilson S.R., Charboneau J.W., Johnson J.A. (2004), *Diagnostic Ultrasound*, Mosby, ISBN 0323020232.

Smutek D., Sara R., Sucharda P., Tjahjadi T., Svec M. (2003), *Image texture analysis of sonograms in chronic inflammations of thyroid gland*, Ultrasound in Medicine and Biology, vol. 29, pp. 1531– 1543.

Theodoridis S., Koutroumbas K. (1999), *Pattern Recognition*, Academic Press, ISBN 0-12-686140-4.

Yoshida H., Casalino D.D., Keserci B., Coskun A., Ozturk O., Savranlar A. (2003), *Wavelet-packet-based texture analysis for differentiation between benign and malignant liver tumours in ultrasound images*, Physics In Medicine and Biology, vol. 48, pp. 3735-3753.